Anal. Chem. **2002,** *74,* 871−878

Surface Characterization of Laser-Ablated Polymers Used for Microfluidics

D. L. Pugmire,*,† E. A. Waddell,† R. Haasch,‡ M. J. Tarlov,† and L. E. Locascio†

National Institute of Standards and Technology, Gaithersburg, Maryland 20899, and Center for Microanalysis of Materials, University of Illinois at Urbana−Champaign, Urbana, Illinois 61801

Fabrication of microfluidic devices by excimer laser ablation under different atmospheres may provide variations in polymer microchannel surface characteristics. The surface chemistry and electroosmotic (EO) mobility of polymer microchannels laser ablated under different atmospheres were studied by X-ray photoelectron spectroscopy and current monitoring mobility measurements, respectively. The ablated surfaces of PMMA were very similar to the native material, regardless of ablation atmospheres due to the negligible absorption of 248-nm light by that polymer. The substrates studied that exhibit nonnegligible absorption at this energy, namely, poly(ethylene terephthalate glycol), poly(vinyl chloride), and poly(carbonate), showed significant changes in surface chemistry and EO mobility when the ablation atmospheres were varied. Ablation of these three polymer substrates under nitrogen or argon resulted in low EO mobilities with a loss of the well-defined chemical structures of the native surfaces, while ablation under oxygen yielded surfaces that retained native chemical structures and supported higher EO mobilities.

Polymeric materials are receiving increasing attention as substrates for microfluidic devices. Polymers possess a range of chemical, physical, and surface properties that allow great flexibility in matching materials to specific device applications. The cost of polymer substrates also can be significantly less than that of glass or silicon.[1] In addition, fabrication of microchannels in polymer substrates is relatively simple and a greater variety of channel geometries, including complex 3-D systems,[2] can be achieved in comparison to glass and silicon substrates.[3,4]

There are many techniques employed for the fabrication of microchannels in polymer substrates including imprinting, etching, casting, and injection molding.[3,4] While these methods are easily implemented, they require fabrication of a template, mask, or mold, otherwise known as a master. The creation of a master is time-consuming and adds an additional step to the microchannel fabrication process. Moreover, minor modifications to the design of a microchannel device require the fabrication of a completely new master.

To circumvent these problems, we are investigating laser ablation as a method for forming microchannels for rapid prototyping of different microfluidic geometries. Another potential feature of laser ablation is the capability of surface modification of channel walls concurrent with microchannel formation.[5] Many reactive species are formed both at the polymer surface and in the gas phase during the laser ablation process. The incorporation or reaction of these ablation products at the nascent channel walls can result in surface chemical functionality that is significantly different from that in the bulk of the polymer.[6] Incorporation of nitrogen or oxygen can give rise to amino, hydroxyl, carboxylic, or phenolic functional groups at the surface.[7] These types of surface functionalities are thought to play an important role in electroosmotic flow (EOF), a commonly used means to pump solution through microchannels.[8,9] The EO mobility of a microfluidic device is directly proportional to the fixed charge that the channel walls possess.[10] The ability to control precisely the type and density of ionizable surface groups, which is usually modulated by application of coatings such as polyelectrolyte monolayers,[8] would allow the tuning of EOF behavior and ultimately lead to more reproducible device performance. Native polymer devices typically have anionic surfaces,[10] resulting in EOF from the anode to cathode. The negative charge is often attributed to carboxylate (COO^-) functionalities, which are the charged groups most likely to be present in polymers containing ester (COO) or carbonate (OCOO) groups.

This paper presents a study of the surface chemistry and electroosmotic flow characteristics of microchannels ablated in poly(ethylene terephthalate glycol) (PETG), polycarbonate (PC), poly(vinyl chloride) (PVC), and poly(methyl methacrylate) (PMMA) under a variety of atmospheres. The goals of this work were to (1) correlate surface chemical properties of the laser-ablated

* Corresponding author: (e-mail) pugmire@nist.gov; (fax) 301-975-2643.
† National Institute of Standards and Technology.
‡ University of Illinois at Urbana−Champaign.

(1) Becker, H.; Gartner, C. *Electrophoresis* **2000**, *21*, 12−26.
(2) Anderson, J. R.; Chiu, D. T.; Jackman, R. J.; Cherniavskaya, O.; McDonald, J. C.; Wu, H.; Whitesides, S. H.; Whitesides, G. M. *Anal. Chem.* **2000**, *72*, 3158−3164.
(3) Becker, H.; Locascio, L. E. *Talanta*. In press.
(4) Soper, S. A.; Ford, S. M.; Qi, S.; McCarley, R. L.; Kelly, K.; Murphy, M. C. *Anal. Chem.* **2000**, *72*, 643A−651A.
(5) Johnson, T. J.; Ross, D.; Gaitan, M.; Locascio, L. E. *Anal. Chem.* **2001**, *73*, 3656−3661.
(6) Chtaib, M.; Roberfroid, E. M.; Novis, Y.; Pireaux, J. J.; Caudano, R.; Lutgen, P.; Feyder, G. *J. Vac. Sci. Technol. A* **1989**, *7*, 3233−3237.
(7) Roberts, M. A.; Rossier, J. S.; Bercier, P.; Girault, H. *Anal. Chem.* **1997**, *69*, 2035−2042.
(8) Barker, S. L. R.; Ross, D.; Tarlov, M. J.; Gaitan, M.; Locascio, L. E. *Anal. Chem.* **2000**, *72*, 5925−5929.
(9) Culbertson, C. T.; Jacobson, S. C.; Ramsey, J. M. *Anal. Chem.* **2000**, *72*, 5814−5819.
(10) Figeys, D.; Pinto, D. *Anal. Chem.* **2000**, *72*, 330A−335A.

10.1021/ac011026r CCC: $22.00
Published on Web 01/09/2002

polymer substrates with their associated microfluidic behavior and (2) determine to what extent changing the local ablation environment alters surface characteristics and associated EOF of these polymers. The latter is attractive because it would allow the fabrication of microchannels in the same substrate with different EOF characteristics. Presently, the most commonly used method to produce microchannels with different EOF characteristics in the same substrate is to adsorb materials to the channel walls that change the surface charge, such as polyelectrolyte monolayers (PEMs).[11,12] While there are many reports of laser ablation of polymers,[6,7,13−26] none have focused on changing the ablation atmosphere for controlling surface characteristics in regard to EOF behavior in microfluidic devices.

EXPERIMENTAL SECTION

Sample Preparation. PETG (DSM Engineering Plastic Products, Sheffield, MA), PC (McMaster-Carr Supply Co., Dayton, NJ), PVC (McMaster-Carr Supply Co.), and PMMA (ICI Acrylics, Memphis, TN) samples were cut to size, sonicated in a 1:1 mixture of ethanol and water, and dried in a stream of dry nitrogen prior to ablation. Samples were prepared for X-ray photoelectron spectroscopy (XPS) analysis by ablation of 0.5 cm by 0.5 cm patches under various atmospheres in the polymer of interest. Analysis of large-area patches, rather than microfluidic channels, was necessary for reasonable XPS signal intensities and data acquisition times. Native plastic samples were prepared by mechanically scraping a piece of the material to expose fresh polymer. Following ablation, samples were stored in air and typically were analyzed with XPS within two to three days.

Information to note about PETG: The chemical structure for the monomer unit is identical to that of poly(ethylene terephthalate) (PET). The reason that the two polymers are differentiated is that PETG is actually a copolymer, having a small amount of a cyclohexane-containing unit added during the production of the plastic as a stabilizer.[27] This becomes an important consideration because the additive may give rise to higher than expected carbon concentrations, especially carbon with binding energies very similar to hydrocarbons in the XPS analysis of PETG samples.

Laser Ablation. A LMT-4000 laser micromachining system (Potomac Photonics, Inc., Lanham, MD) equipped with a KrF pulsed (7 ns) excimer laser, operating at 248 nm, together with an Unidex 500 PC-based motion controller (Aerotech, Pittsburgh, PA) were used for ablating polymer samples. It was possible to control the repetition rate of the laser from single shot to 200 Hz, and the programmable motorized stage had a ±1-μm repeatability. The micromachining system was equipped with real-time live video software that enabled visualization of the ablation process. Laser fluences of 40.0 and 408 mJ/cm^2 and substrate feed rates of 10 and 1 mm/s were used to produce the XPS and EOF samples, respectively. XPS samples were prepared differently from EOF samples to increase the concentration of chemically modified material at the sample surface,[28,29] enhancing the signal related to the ablated polymer material during XPS studies. These differences in sample preparation do not greatly affect the chemistry of the ablated surface,[28−31] thereby still allowing a qualitative comparison of the two data sets.

Ablation under a particular atmosphere was performed with a nozzle directing the desired gas at the sample/laser intersection. The ablation gases, oxygen (99.6%), nitrogen (liquid N_2 boil-off), and argon (99.999%), were used. It should be noted that this ablation procedure resulted in an environment that was not contained. Therefore, incorporation of a small amount of air into the desired ablation atmosphere may have been possible.

XPS Analysis. The XPS data were collected on an Axis Ultra (Kratos Analytical) spectrometer using monochromatized Al Kα radiation (1486.6 eV) with a power of 300 W. Survey spectra were typically an average of three scans with 1 eV/step and were acquired at a pass energy of 160 eV. High-resolution spectra of C 1s, O 1s, and Cl 2p were typically acquired by averaging five scans at 0.1 eV/step and a pass energy of 40 eV. The dwell time for all spectra was 100 ms. A charge neutralizer with filament current of 1.8 A, charge balance of 2.54 V, and filament bias of 1 V was used to reduce charging of the nonconducting polymer samples. Binding energy corrections were made by referencing the aromatic carbon of PETG to 284.7 eV[32] and of PC to 284.5 eV,[32] the methyl carbons of PMMA to 285.0 eV,[32] and the carbon not directly bound to chlorine of PVC to 285.9 eV.[32] Relative atomic concentrations were determined by integrating spectra that were fit with Gaussian-profile peak shapes after subtraction of a Shirley-type background.[33] The sensitivity factors employed here for comparison of heteroatomic concentrations were provided by the instrument manufacturer and are as follows: $S_{C\ 1s} = 0.278$, $S_{O\ 1s} = 0.780$, $S_{N\ 1s} = 0.477$, $S_{Cl\ 2p} = 0.891$, and $S_{Sn\ 3d} = 7.875$. The COOX concentrations discussed below were determined by integrating the carbon 1s envelope at binding energies above 288.7 eV, the typical energy region for COOX groups.[32] Error due

(11) Barker, S. L. R.; Tarlov, M. J.; Canavan, H.; Hickman, J. J.; Locascio, L. E. *Anal. Chem.* **2000**, *72*, 4899−4903.
(12) Chen, W.; McCarthy, T. J. *Macromolecules* **1997**, *30*, 78−86.
(13) Burrell, M. C.; Liu, Y. S.; Cole, H. S. *J. Vac. Sci. Technol. A* **1986**, *4*, 2459−2462.
(14) Feng, Y.; Liu, Z. Q.; Yi, X.-S. *Appl. Surf. Sci.* **2000**, *156*, 177−182.
(15) Lazare, S.; Lopez, J.; Weisbuch, F. *Appl. Phys. A* **1999**, *69*, S1−S6.
(16) Lemoine, P.; Cazzini, K.; McGovern, I. T.; Blau, W. J.; Batz, P.; Ziegler, C.; Gopel, W. *Chem. Phys. Lett.* **1994**, *220*, 177−180.
(17) Lippert, T.; Webb, R. L.; Langford, S. C.; Dickinson, J. T. *J. Appl. Phys.* **1999**, *85*, 1838−1847.
(18) Krajnovich, D. J. *J. Phys. Chem. A* **1997**, *101*, 2033−2039.
(19) Blanchet, G. B.; Fincher, C. R. *Appl. Phys. Lett.* **1994**, *65*, 1311−1313.
(20) Hemmerlin, M.; Mermet, J. M. *Spectrosc. Acta Pt. B−At. Spectrosc.* **1997**, *52*, 1687−1694.
(21) Srinivasan, R.; Braren, B. *Chem. Rev.* **1989**, *89*, 1303−1316.
(22) Devalckenaere, M.; Jadin, A.; Kolev, K.; Laude, L. D. *Nucl. Instrum. Methods Phys. Res. Sect. B−Beam Interact. Mater. At.* **1999**, *151*, 263−267.
(23) Schnyder, B.; Wambach, J.; Kunz, T.; Hahn, C.; Kotz, R. *J. Electron Spectrosc. Relat. Phenom.* **1999**, *105*, 113−117.
(24) Kreutz, E. W.; Frerichs, H.; Stricker, J.; Wesner, D. A. *Nucl. Instrum. Methods Phys. Res. Sect. B−Beam Interact. Mater. At.* **1995**, *105*, 245−249.
(25) Viville, P.; Beauvois, S.; Lambin, G.; Lazzaroni, R.; Bredas, J. L.; Kolev, K.; Laude, L. *Appl. Surf. Sci.* **1996**, *96−8*, 558−562.
(26) Niino, H.; Yabe, A. *Appl. Surf. Sci.* **1996**, *96−8*, 572−576.
(27) Oh, T. S.; Ryou, J. H.; Chun, Y. S.; Kim, W. N. *Polym. Eng. Sci.* **1997**, *37*, 838−844.
(28) Bianchi, F.; Chevolot, Y.; Mathieu, H. J.; Girault, H. H. *Anal. Chem.* **2001**, *73*, 3845−3853.
(29) Johnson, T. J.; Waddell, E. A.; Kramer, G. W.; Locascio, L. E. *Appl. Surf. Sci.* **2001**, *181*, 149−159.
(30) Lazare, S.; Hoh, P. D.; Baker, J. M.; Srinivasan, R. *J. Am. Chem. Soc.* **1984**, *106*, 4288−4290.
(31) Lazare, S.; Srinivasan, R. *J. Phys. Chem.* **1986**, *90*, 2124−2131.
(32) Beamson, G.; Briggs, D. *High-Resolution XPS of Organic Polymers: The Scienta ESCA300 Database*; John Wiley & Sons: New York, 1992.
(33) Shirley, D. A. *Phys. Rev. B* **1972**, *5*, 4709−4714.

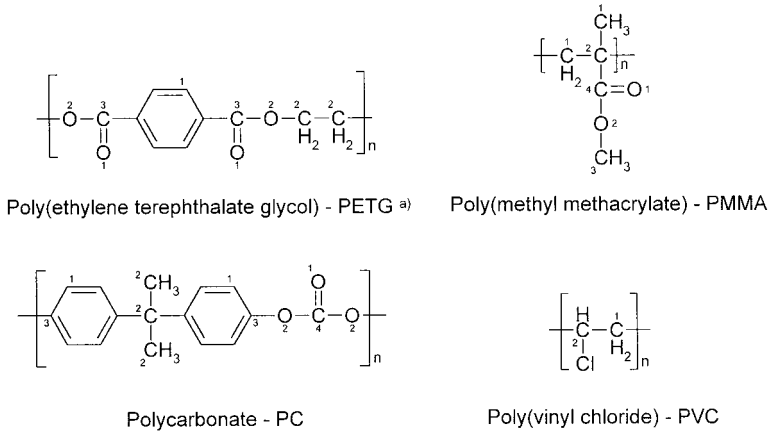

Figure 1. Chemical structures of polymers investigated in the present study. a)Monomer structure of the major component of PETG. See text.

to the data-fitting procedure is estimated to be 2% for relative atomic concentration ratios and 5% for COOX/C concentration ratios. Spectra of each sample of a particular substrate material were collected in the same order to ensure the same amount of X-ray exposure during each stage of data collection and thereby minimize effects of X-ray damage on comparing relative concentrations between samples.

EOF Measurements. The electroosmotic mobility measurements were made with the current monitoring method as described elsewhere[34] and are briefly described here. Poly(dimethylsiloxane) (PDMS) lids used to seal ablated channels were produced by mixing Sylgard 184 curing agent with Sylgard 184 Silicone Elastomer (Dow Corning Corp., Midland, MI) in a 10:1 ratio and allowing the mix to cure for several days. Two through holes (reservoirs), each 3 mm in diameter, were cut into the lids at either end of a 2-cm channel. The channel was then vacuum-filled with a 0.020 mol/L, pH 7.0 phosphate buffer (potassium dihydrogenphosphate and disodium phosphate, Sigma-Aldrich, St. Louis, MO). An electric potential was applied across the channel via platinum electrodes inserted into each hole. After current stabilization, the buffer was removed from one reservoir and replaced with 0.010 mol/L, pH 7.0 phosphate buffer. The current was then monitored and allowed to plateau. Dividing the length of the microchannel by the time required for the channel to fill with the less concentrated buffer yielded the electroosmotic flow velocity and dividing this result by the field strength gave the electroosmotic mobility. For the present study, field strengths of 50−250 V/cm were used, generating a maximum current of 5 μA. At these field strengths, we have determined that Joule heating is negligible.

RESULTS AND DISCUSSION

The nominal chemical structures of the polymers employed in the present study are shown in Figure 1. Previous investigations of laser-ablated polymers provide clues to the expected behavior of the polymers used in the current study.[15,35] In general, the ablation characteristics will depend strongly on whether the polymer absorbs at the wavelength of the incident radiation. PETG and PC are strong and moderate absorbers, respectively, at 248 nm, while the absorbance of PMMA at this wavelength is negligible.[15] Pure PVC also does not absorb at this wavelength; however, conjugated diene (C═C−C═C) decomposition products naturally present in PVC are strong UV absorbers.[35] Materials that strongly absorb ablation radiation, such as PETG, PC, and PVC, are susceptible to surface photochemistry and ablate relatively slowly, while weak absorbers, such as PMMA, ablate quickly by explosive thermal mechanisms but are not as susceptible to chemical changes in the surface.[14,15]

Table 1. Concentration Ratios As Determined by XPS and EO Mobilities of Polymers Ablated under Various Atmospheres

	native	argon	nitrogen	oxygen	expected[a]
			PMMA		
O/C	0.37	0.36	0.36	0.46	0.40
COOX/C	0.19	0.17	0.17	0.20	0.20
EO mobility	na[b]	na	na	na	na
			PETG		
O/C	0.33	0.34	0.34	0.55	0.40
COOX/C	0.14	0.10	0.10	0.20	0.20
EO mobility	na	5.02 ± 0.97[c]	4.37 ± 0.65[c]	6.28 ± 0.71[c]	na
			PVC		
O/C	0.01	0.27	0.31	0.53	0.00
COOX/C	0.00	0.10	0.11	0.20	0.00
EO mobility	na	3.53 ± 0.64[c]	4.38 ± 0.91[c]	5.24 ± 0.86[c]	na
			PC		
O/C	0.19	0.39	0.40	0.26	0.19
COOX/C	0.09	0.12	0.13	0.06	0.06
EO mobility	na	3.71 ± 0.45[c]	2.84 ± 0.41[c]	5.29 ± 1.01[c]	na

[a] Concentration ratios expected from monomer unit stoichiometry. [b] na, not available. [c] All EO mobilities reported in units of 10^{-4} $cm^2/V{\cdot}s$.

EO mobilities in laser-ablated channels were studied to evaluate changes in the microchannel surfaces ablated under different atmospheres. EO mobility correlates directly with ζ-potential and, therefore, surface charge density in microfluidic channels. The EO mobility study is summarized in Table 1 where mobilities for PETG, PVC, and PC ablated under argon, nitrogen, and oxygen are reported. When considering these EO mobility data, one should keep in mind that the top wall of each microfluidic channel is PDMS, which will have an effect on the EO mobility. However, this effect will be the same for all ablated channels in all materials studied and thus may be neglected in a qualitative comparison of

(34) Locascio, L. E.; Perso, C. E.; Lee, C. S. *J. Chromatogr., A* **1999**, *857*, 275−284.
(35) Izumi, Y.; Kawanishi, S.; Suzuki, N.; Maruo, M.; Ichinose, N.; Yamamoto, T. *Bull. Chem. Soc. Jpn.* **1997**, *70*, 2855−2859.

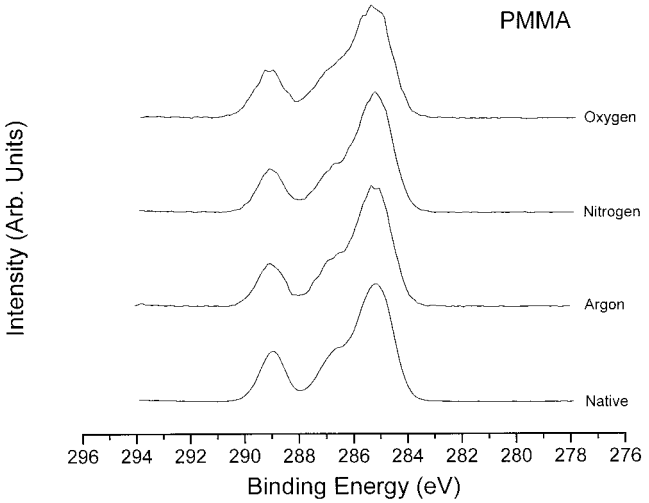

Figure 2. C 1s XP spectra of native PMMA and PMMA ablated under nitrogen, argon, or oxygen. Spectra very similar to the native sample are obtained regardless of the ablation atmosphere.

the EO mobility to surface chemistry of ablated microchannels. As will be discussed below, determination of the EO mobility of PMMA samples was not possible. In general, the data indicate that ablation under oxygen results in devices with higher EO mobilities than those ablated under argon or nitrogen. This trend is expected, assuming that ablation under oxygen yields higher surface oxygen concentrations and that the COO^- surface concentration is proportional to the surface oxygen concentration. X-ray photoelectron spectroscopy was used in this study to examine this hypothesis. We first present the XPS results obtained from the various polymers ablated under different atmospheres and then discuss the relationship between the EO mobilities and the surface properties as determined by XPS.

PMMA. Unfortunately, it was not possible to determine the EO mobility of ablated microchannels in PMMA by the current monitoring technique, as a stable baseline measurement could not be consistently obtained. We attribute the unstable flow to cracking of the channel walls and debris in the channel, which was observed with scanning electron microscopy (not shown). Presumably, these topological features result from the thermal ablation-like mechanism for PMMA at this wavelength.[13,14] Although PMMA ablation under various atmospheres is not expected to result in significant chemical changes of the surface,[13] XPS analysis is nonetheless useful for comparing to substrates that might exhibit chemical changes at the surface upon ablation.

The C 1s XP spectra of native PMMA and PMMA ablated under argon, nitrogen, and oxygen are shown in Figure 2. The intensities are normalized to the integrated intensity of the carbon backbone, C(1) and C(2) in Figure 1, centered at 285.0 eV. Noteworthy is that the C ls spectra appear similar for all ablation environments. The C 1s and O 1s binding energies, reported in Table 2 are nearly identical for all of the spectra as well and are similar to values previously reported.[32] The total oxygen to total carbon (O/C) concentration ratios are reported in Table 1 and are close to that expected from the stoichiometry of the monomer unit. Ablation of PMMA under argon or nitrogen does not result in a significant change in the O/C, although ablation under oxygen results in a small uptake of oxygen. This small increase in oxygen content is manifested in the C 1s spectrum, where a slight increase

Table 2. Observed Binding Energies (in eV) of Polymers Ablated under Various Atmospheres

	native	argon	nitrogen	oxygen	lit.[a]
			PMMA		
C(1)	285.0	285.0	285.0	285.0	285.0
C(2)	285.7	285.7	285.6	285.8	285.7
C(3)	286.8	286.8	286.8	286.9	286.8
C(4)	289.0	289.0	289.0	289.1	289.0
O(1)	532.2	532.2	532.2	532.2	532.2
O(2)	533.7	533.8	533.8	533.7	533.8
			PETG		
C(1)	284.7	284.7	284.7	284.7	284.7
C(2)	286.2	286.4	286.4	286.4	286.2
C(3)	288.7			288.8	288.7
O(1)	531.7	531.8	531.8	531.6	531.6
O(2)	533.3	533.3	533.3	533.2	533.2
			PVC		
C(1)	285.9	285.9	285.9	285.9	285.9
C(2)	287.1			287.4	287.0
Cl $2p_{3/2}$	200.8	201.4	201.3	201.1	200.6
Cl $2p_{1/2}$	202.4	203.0	203.0	202.8	202.3
			PC		
C(1)	284.5	284.5	284.5	284.5	284.5
C(2)	285.0	285.0	285.0	285.0	285.0
C(3)	286.2	286.3	286.3	286.3	286.2
C(4)	290.5			290.4	290.4
O(1)	532.3	532.2	532.1	532.0	532.3
O(2)	534.0	533.9	533.9	533.9	534.0

[a] Previously reported native polymer binding energies are from ref 32.

in the relative concentrations of C(3) and C(4) oxygen-bonded carbon atoms is observed. While there are minor chemical changes for the oxygen-ablated PMMA, it is clear that the polymer surface remains largely unchanged in the three ablation environments studied. These results are consistent with a thermal ablation mechanism for PMMA whereby material ejection occurs without significant chemical bond rupture and a previous study that found small variations in surface charge upon ablation of PMMA under nitrogen and oxygen.[29]

PETG. The C 1s XP spectra of native PETG and PETG ablated under various atmospheres are shown in Figure 3. The intensities are normalized to those of the aromatic carbon signal in each spectrum, C(1) in Figure 1. In contrast to the behavior observed for PMMA, the C 1s XP spectra for argon and nitrogen ablation environments are significantly different from the native PETG spectrum. The PETG C 1s binding energies and O/C concentration ratios are reported in Tables 1 and 2, respectively.

The binding energies of the native polymer are similar to those reported previously for PET.[32] However, the total O/C ratio, as well as the concentrations of C(2) and C(3) relative to C(1), appears to be lower than what is expected from the monomer stoichiometry. These discrepancies can be accounted for by contributions from cyclohexane-containing additives incorporated into PETG as discussed previously. Aliphatic hydrocarbons, such as cyclohexane, typically appear at C 1s binding energies of 285.0 eV,[32] close to the 284.7 eV binding energy of C(1) in PET or PETG. Therefore, the high relative intensity of the C(1) feature and lower than expected O/C ratio may result from aliphatic additives in PET.

When ablated in an argon environment, the C 1s XP spectrum of PETG is markedly different from that obtained for native PETG.

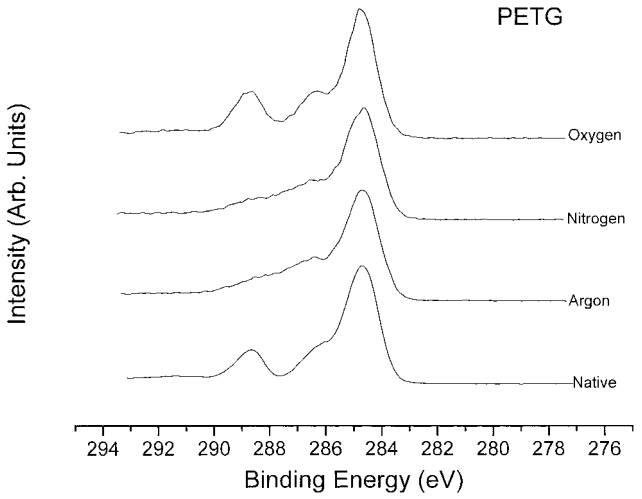

Figure 3. C 1s XP spectra of native PETG and PETG ablated under various atmospheres. Oxygen ablation yields a spectrum similar to native PETG; however, argon and nitrogen ablation give very different results.

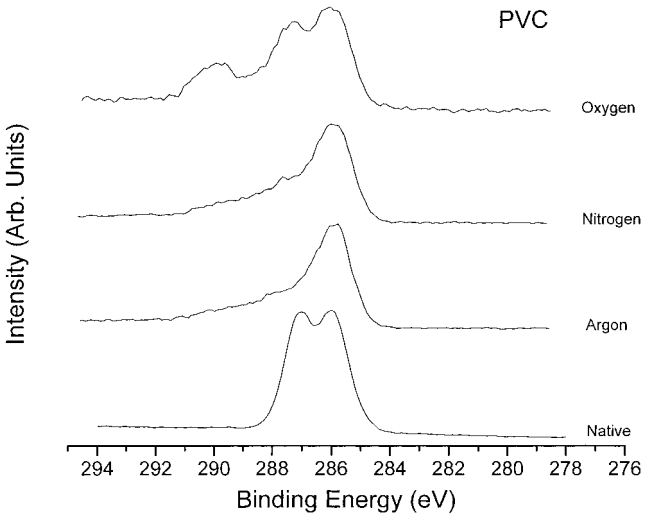

Figure 4. C 1s spectra of native PVC and PVC ablated under nitrogen, argon, or oxygen. Ablation under inert argon or nitrogen atmospheres results in loss of the 287.1 eV feature due to carbon bonded to chlorine.

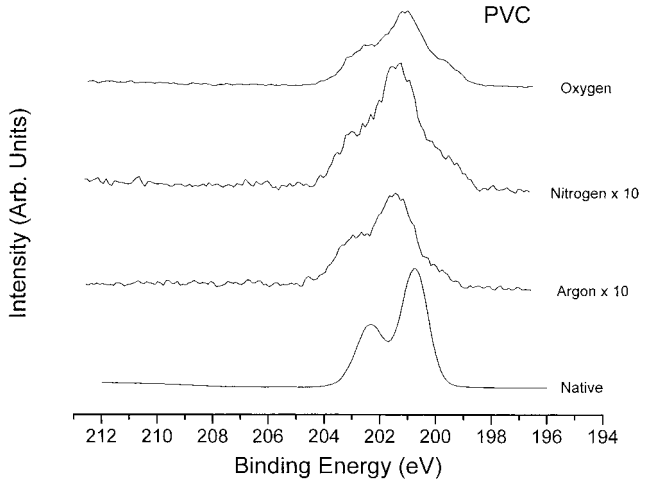

Figure 5. Cl 2p XP spectra of native PVC and PVC ablated under various atmospheres. The argon and nitrogen spectra have been multiplied by 10 in order to display them with the other spectra.

The most apparent difference is the great reduction in the relative intensity of the well-defined ester (COO, C(3)) carbon peak centered at 288.7 eV. The spectrum now appears as an aromatic-type carbon peak and a broad tail to the high-energy side. While the origin of the tail cannot be unequivocally assigned, it is reasonable to assume that its appearance is indicative of various oxidized carbon species such as alcohols, ethers, carbonyls, carboxylic acids, and esters, all of which could contribute to the C 1s spectrum in the region of the observed high-energy tail, and that there seems to be no selective enrichment of any particular functional group. While the O/C ratio of 0.34 is similar to that observed for the native PETG sample, it is evident from the C 1s XP spectra that significant chemical changes have occurred when compared to the native surface. The broad higher binding energy tail of the C 1s spectrum suggests that the well-defined chemical structure of the bulk polymer has been lost and that a range of different oxygen-containing functionalities has formed at the surface. As seen in Figure 3, almost identical results are found when PETG is ablated under a nitrogen atmosphere.

Ablation of PETG under O_2 yields a C 1s XP spectrum that is nearly identical to that of the native plastic. The O/C ratio increases to a value of 0.55, indicating a significant increase in the surface oxygen concentration. A peak not observed for the native polymer in the O 1s XP spectrum (not shown) appears at 532.4 eV, located between the two types of oxygen observed in the N_2- and Ar-ablated polymers, and accounts for most of the observed increase in the O/C ratio. The energy of this new peak in the O 1s spectrum is indicative of the formation of carboxylic acid, or alcohol OH groups, or both,[32] an interpretation consistent with the corresponding increase in the amount of COOX (X = H or C) carbon in the C 1s spectrum.

PVC. The C 1s XP spectra of native PVC and samples ablated under Ar, N_2, and O_2 are shown in Figure 4, and associated binding energies are given in Table 2. As expected, the spectrum of the native material shows two chemically distinct carbon peaks of nearly equal intensity where the higher energy peak, C(2), is due to carbon atoms bound directly to chlorine. The O 1s spectrum (not shown) reveals a small amount of surface oxygen (total O/C ratio <0.01). The minor surface oxygen component is due either to incorporation of a small amount of oxygen during production of the plastic, adsorption of oxygen-containing contaminants or to oxidation of the PVC surface in the short time between mechanical scraping and introduction into vacuum. In Figure 5, the Cl 2p spectrum exhibits the Cl $2p_{3/2}/2p_{1/2}$ doublet at energies expected for PVC. These results are all consistent with a relatively pristine, bulklike PVC surface.

Ablation of the PVC substrate under argon and nitrogen yields XP spectra of nearly identical peak shapes and intensities so these results are discussed collectively. The C 1s spectra of the argon- or nitrogen-ablated samples are shown in Figure 4. They consist of a predominant, hydrocarbon-like peak centered at 285.9 eV and a broad, high binding energy tail. The higher binding energy peak due to carbon bound to chlorine, C(2), easily resolved in the native sample, is now significantly diminished in intensity and no longer resolved. It is interesting to note that the C 1s spectra of the argon- and nitrogen-ablated PVC resemble those of PETG ablated in the same environments. As such, we interpret the high binding energy

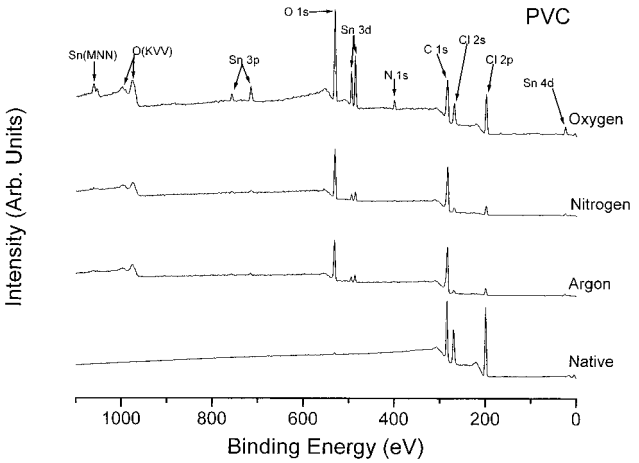

Figure 6. Survey spectra of native PVC and PVC ablated under nitrogen, argon, or oxygen. Ablation of PVC results in loss of Cl, uptake of O, and appearance of Sn; see text for discussion.

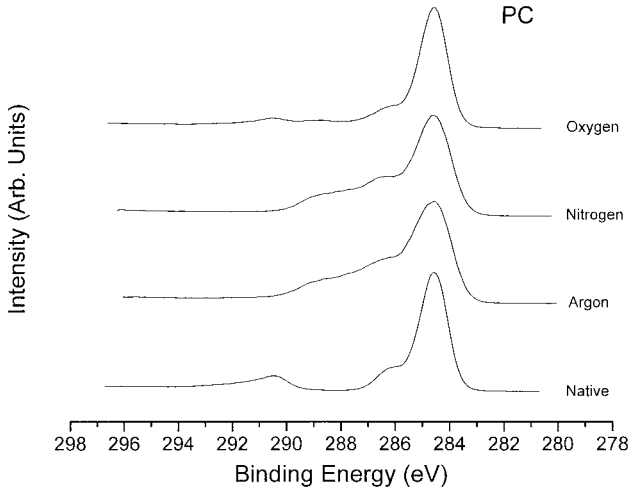

Figure 7. C 1s XP spectra of native PC and PC ablated under various atmospheres. Ablation under argon and nitrogen yields spectra similar to PETG and PVC ablated under similar atmospheres.

tail of PVC in the same way as for PETG, i.e., as incorporation of a wide variety of oxygen-containing functionalities, although there are likely some contributions to the peak envelope from chlorine-containing substituents. Supporting this view is the observed increase in the amount of oxygen at the PVC surface. The O/C ratio of the argon- and nitrogen-ablated PVC samples are 0.27 and 0.31, respectively, indicating significant uptake of oxygen relative to the native sample. The increased oxygen amounts observed for ablation under inert argon and nitrogen atmospheres can be explained by the probable formation of reactive surface radicals during ablation and their subsequent reaction with oxygen-containing species upon returning the sample to ambient conditions (i.e., exposure to air) or reaction of the surface with small amounts of oxygen that are possibly present in the ablation atmosphere.

As seen in Figure 5, a sharp decrease in chlorine concentration is also observed upon ablation under argon or nitrogen (Note: The spectra of the samples ablated under argon and nitrogen in Figure 5 have been expanded by 1 order of magnitude.), consistent with the observed decrease in intensity of the C(2) peak in the C 1s spectra. The Cl 2p spectrum also now shows two distinct sets of doublets. The higher energy doublet is attributed to the chlorine remaining in the intact polymer. The origin of the lower energy doublet at 200.0 and 201.6 eV is apparent by examination of the survey XP spectra of native and argon-ablated samples, shown in Figure 6. The survey spectrum, in addition to showing the decrease in chlorine and increase in oxygen as discussed above, also clearly shows the presence of tin in the ablated samples with the Sn 3d peaks located between 480 and 500 eV. We believe that the tin is derived from organotin compounds that are used as photostabilizers in PVC.[20] The ablation process appears to concentrate the tin at the surface because tin is not detected in the native sample. The Sn 3d 5/2 binding energy of 487.4 eV is consistent with the Sn existing in the +2 or +4 valence state. We conclude that the lower energy Cl doublet is therefore attributable to chloride ions that are bound to tin. However, the Cl/Sn intensity ratios (1.03 and 1.83 for Ar and N_2 ablation, respectively) indicate that the chloride concentration is not high enough to bind all of the tin observed, assuming a stoichiometry of $SnCl_4$ or $SnCl_2$. Therefore, the remainder of the tin present in the sample is most likely in the form of a tin oxide as a result of reaction with atmospheric oxygen or water.

Ablation of PVC under oxygen results in a C 1s XP spectrum, shown in Figure 4, much different from those observed for argon, nitrogen, or native samples. A new peak appears at 290.0 eV, indicative of carbon existing as COOX (X = H or C). There is also a corresponding increase in the O/C ratio to 0.53 relative to the nitrogen- or argon-ablated samples. In addition, the C 1s spectrum shows that a significant amount of the native chlorine-bonded carbon, C(2), is retained in this sample. Similarly, the Cl 2p spectrum, Figure 5, indicates the presence of significant concentrations of chlorine, with chlorine bonded to carbon and chlorine bonded to tin as chloride. Along with the large increase in nonpolymeric chlorine when comparing the oxygen-ablated sample to argon- or nitrogen-ablated samples, there is a correspondingly large increase in the amount of tin, as observed in the survey spectrum (Figure 6) of the oxygen-ablated sample. The reason for a higher tin concentration in the oxygen-ablated sample has not been determined.

PC. Shown in Figure 7 are the C 1s XP spectra of native PC and samples ablated under argon, nitrogen, or oxygen. The native plastic spectrum is dominated by a relatively intense peak centered at 284.5 eV that is derived from both aromatic C(1) and aliphatic C(2) carbons, whose binding energies are reported in Table 2. The aromatic carbon, C(3), that is single bonded to one oxygen atom, and the carbonate carbon, C(4), are also observed with binding energies and relative intensities consistent with those expected of PC.[32] The native PC sample also yields an O/C ratio of 0.19, the value expected for this polymer.

As for all the previously discussed polymers, ablation of PC under argon or nitrogen yielded nearly identical XPS spectra so these results are discussed collectively. When PC is ablated under nitrogen and argon, the C 1s XP spectrum observed is similar in shape to those of PETG or PVC samples under the same conditions. The spectral envelope is dominated by an intense C(1) peak at 284.5 eV with tailing to the higher binding energy side. However, the tailing region is slightly more intense than those of PVC or PETG. The carbonate carbon, C(4), observed in the native plastic is greatly diminished, indicating nearly complete removal

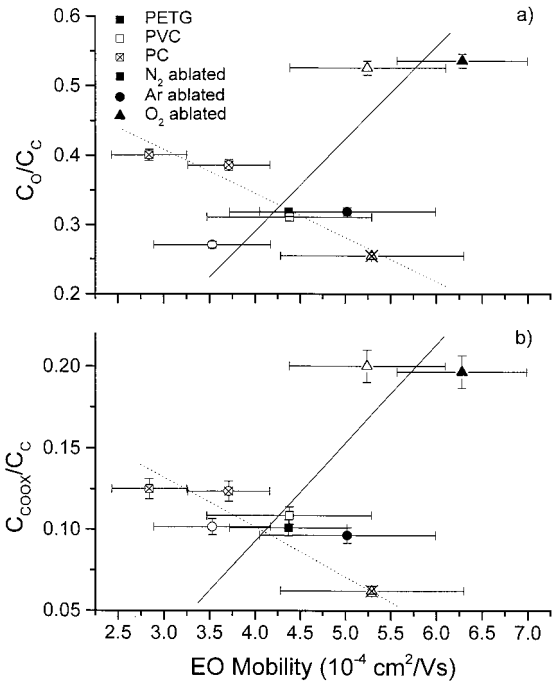

Figure 8. Graphical representations of (a) XPS C_O/C_C ratios and (b) XPS C_{COOX}/C_C ratios versus the corresponding EO mobilities of PETG, PVC, and PC samples. PETG samples are represented in solid symbols, PVC in open symbols, and PC in crossed symbols, with squares representing ablation under N_2, circles representing ablation under Ar, and triangles representing ablation under oxygen. The lines are included strictly as guides to the eye and denote the two different classes of behaviors observed for the polymers studied.

of this functionality at the surface. Surprisingly, the O/C ratio increases to 0.39, significantly higher than the value of 0.19 observed for the native PC. Although the well-defined carbonate peak is lost upon inert gas ablation, the relative overall amount of COOX carbon has increased, as reported in Table 1.

Unlike the other substrates studied, ablation of PC under oxygen results in an O/C ratio (0.26) that is lower than the argon- or nitrogen-ablated PC samples. The lower O/C ratio is accompanied by a relatively lower amount of oxygen functionalities observed in the C 1s region between 285.5 and 290.0 eV. The lower oxygen concentrations present in this sample may possibly be due to the formation and subsequent loss of CO, CO_2, or both during ablation in this oxygen-rich environment. In contrast to the inert gas-ablated PC, the oxygen-ablated PC exhibits a carbonate feature at 290.4 eV. At first glance, the C 1s region of the oxygen-ablated PC appears almost identical to that of the native PC; however, there are a number of subtle differences. The relative amounts of the native oxidized carbon, C(3) and C(4), are lower, indicating that the carbonate concentration decreases upon oxygen ablation. Moreover, the spectrum shows the appearance of a small feature at 289.0 eV, a binding energy consistent with the presence of COOX (X = H or C).

Relationship between EO Mobilities and Surface Properties. The XPS and EOF data are presented graphically in Figure 8, which contains plots of the XPS O/C ratio versus the EO mobility (Figure 8a) and the COOX/C ratio (where X = H or C) versus the EO mobility (Figure 8b) for PETG, PVC, and PC. The lines in Figure 8 are included strictly as guides to the eye and denote the two different classes of behavior observed for these polymers. Although there are significant uncertainties in the measurement of the EO mobilities, the general trend that emerges for PETG and PVC is that surfaces with higher oxygen content exhibit higher EO mobilities. For example, the highest O/C ratios (0.53−0.55) for PETG and PVC are obtained for ablation under an oxygen atmosphere and the corresponding EO mobilities fall in the range of 5.25×10^{-4}−6.5×10^{-4} cm^2/V·s. Conversely, the lower O/C ratios (0.27−0.34) obtained for ablation of PETG and PVC under Ar or N_2 result in a correspondingly lower range of EO mobilities, 3.5×10^{-4}−5.0×10^{-4} cm^2/V·s.

The behavior observed for PC is the opposite of that observed for PETG and PVC in two respects. First, ablation under atmospheres of N_2 or Ar results in surfaces with higher O/C ratios (0.39−0.40) than ablation under oxygen (0.26). Second, surfaces with higher oxygen content from inert gas ablation yield lower EO mobilities (2.8×10^{-4}−3.7×10^{-4} cm^2/V·s) than the lower oxygen content surface from oxygen ablation (5.3×10^{-4} cm^2/V·s). We note that the O/C ratio may not accurately reflect the surface density of charged species because it is unlikely that all oxygen-containing functional groups carry negative charge. Since carboxylate groups are more likely to be negatively charged, the ratio of carboxylate groups to total carbon, COOX/C (where X = H or C), was also plotted against the EO mobility in Figure 8b. While there are some minor differences between the plots of COOX/C and O/C versus EO mobility, the general trends are the same. We thus conclude that there is no simple, direct correlation of total oxygen concentration or COOX moiety concentration with the EO mobility of polymeric microchannels fabricated by laser ablation.

There are several possible reasons why a simple correlation between surface oxygen and EO mobility is not found. One possibility is the different environments that the XPS and EO mobility studies were performed under. The ultrahigh-vacuum conditions necessary for XPS are likely to result in surface conditions that are different from those present in a buffer solution, considering that surface charge can vary significantly even with changes in pH. Another possibility is that other surface species besides those containing oxygen carry charge. For example, nitrogen-containing moieties were observed in some of the samples analyzed in the present study. The top spectrum of Figure 6, the survey scan of PVC ablated in oxygen, shows N 1s intensity at approximately 400 eV. The binding energies of all nitrogen observed in this study were typically found in the high-resolution spectra at 399.6 and 401.7 eV, respectively (not shown), consistent with NR_xH_y ($x + y = 3$) and $NR_xH_y^+$ ($x + y = 4$). These are surface groups that either have a native positive charge or are capable of carrying a positive charge. As COO groups are negatively charged, these nitrogen-containing groups are expected to decrease the EO mobility. In the cases of PETG and PVC, the oxygen-ablated samples incorporated the most nitrogen, with the argon and nitrogen samples having undetectable, or nearly undetectable, amounts of nitrogen present. The PC samples, in which the oxygen concentration trend was different from that observed for PETG and PVC, have the opposite trend for nitrogen incorporation as well. The argon and nitrogen ablated samples had N to C concentration ratios that were 3−4 times higher than what was observed for the O_2-ablated sample. Thus, the greater concentrations of positively charged nitrogen-containing surface species may

counterbalance the higher O and COOX concentrations and result in the lower than expected EO mobilities for argon- and nitrogen-ablated PC samples.

CONCLUSIONS

These studies demonstrate that the surface properties and electroosmotic mobility of microchannels formed in polymer substrates can be altered in a one-step process by changing the atmosphere under which laser ablation is performed, eliminating the need for coatings. For the polymers studied, ablation under oxygen yielded microchannels with higher EO mobilities in comparison to ablation under argon and nitrogen. PETG, PVC, and PC, which ablate via a photochemical mechanism, exhibit significant differences in surface chemical compositions depending on whether polymers were ablated under inert gas or oxygen atmospheres. In contrast, the surface composition of PMMA, which ablates via a thermal mechanism, did not vary significantly when ablated under different atmospheres. Various species were identified from XPS that could potentially carry surface charge and directly support EO flow, including oxygen- and nitrogen-containing moieties; however, a simple correlation between the concentrations of these species and the measured EO mobilities was not apparent. This work also highlights the value of ascertaining the surface chemical composition of the laser-ablated polymers. In the case of PVC, ablation leads to a concentrating at the surface of tin chlorides and oxides. These tin species are presumably derived from trace amounts of organotin complexes added as photostabilizers during the production of PVC. The organotin complexes are not detected by XPS in the bulk PVC. The presence of the surface tin oxides and chloride could potentially be problematic in microfluidic applications, leading to a time-varying EO mobility or contamination of flow streams.

ACKNOWLEDGMENT

The authors thank the Center for Microanalysis of Materials, University of Illinois, which is supported by the U.S. Department of Energy under Grant DEFG02-96-ER45439, for use of the XPS facilities. D.L.P. and E.A.W. acknowledge NRC postdoctoral fellowships at NIST. Certain commercial equipment, instruments, or materials are identified in this paper in order to specify the experimental procedure adequately. Such identification is not intended to imply recommendation or endorsement by the National Institute of Standards and Technology, nor is it intended to imply that the materials or equipment identified are necessarily the best available for the purpose.

Received for review September 24, 2001. Accepted November 27, 2001.

AC011026R